INTEGRATION OF DAMPING PROPERTIES OF ASSEMBLED STRUCTURES INTO THE FINITE ELEMENT METHOD USING THIN-LAYER ELEMENTS AND THE MODEL OF CONSTANT HYSTERESIS

Schmidt, A., Al-Tameemi, H., Bograd, S., Gaul., L.

Institut für Angewandte und Experimentelle Mechanik, Universtät Stuttgart
Pfaffenwaldring 9, 70550 Stuttgart, Germany
schmidt@iam.uni-stuttgart.de

SUMMARY: The vibration and damping characteristics of an assembled structure made of steel are investigated by an experimental modal analysis and compared with the results of a finite element modal analysis. A generic experiment is carried out to evaluate the stiffness and the damping properties of the structure's join patches. Using these results, an appropriate finite element model of the structure is developed where the join patches are represented by thin-layer elements containing material properties which are derived from the generic experiment's results. The joint's stiffness is modeled by orthotropic material behavior whereas the damping properties are represented by the model of constant hysteresis, leading to a complex-valued stiffness matrix. A comparison between the experimental and the numerical modal analysis shows good agreement. An optimization procedure for the joint's stiffness and the damping properties leads to an improved correlation between the experimental and the numerical modal quantities and reveals that the results of the generic experiment are sound.

KEYWORDS: damping, constant hysteresis, finite element method, thin-layer elements.

NOMENCLATURE

EMA	Experimental modal analysis
FEM	Finite element method
TLE	Thin-layer element
i	Imaginay unit
d	Thickness of the TLEs
f^{exp}, f^{FEM}	EMA eigenfrequency, FEM eigenfrequency
k, m	Tangential stiffness, Mass
a, u	Acceleration, Displacement
r, A	Residuum, Contact surface
E, E^*	Young's modulus, Complex Young's modulus
$E_{11}\ldots E_{66}$	Entries of the 3d material matrix
F, G	Force, Shear modulus
W_{d}, $U_{\max}$	Dissipated energy, Maximal stored energy
η, η_{m}	Loss factor, Modal damping in percent
γ, τ, σ, ε	Shear strain, Shear stress, Stress, Strain
λ, λ^*	Real Eigenvalue, Complex Eigenvalue
$\boldsymbol{K}$, $\boldsymbol{K}^*$, $\boldsymbol{M}$	Stiffness matrix, Complex stiffness matrix, Mass matrix
$\boldsymbol{\varphi}$, $\boldsymbol{\varphi}^*$	Real eigenvector, Complex Eigenvector

1. INTRODUCTION

Vibrating mechanical systems assembled from metallic components dissipate energy due to the existence of damping. Besides the loss of energy in the material itself (material damping) especially the join patches contribute to the energy dissipation since microslip within the contact surfaces cannot be avoided. As long as the exciting forces do not exceed a certain level, the damping properties are nearly linear with respect to the excitation level. In addidtion, experimental investigations show that the stiffness and the damping properties of materials as well as those of the joints are nearly frequency independent [1].
For numerical simulations of the dynamical behavior of structures, the finite element method (FEM) has established itself as a common powerful tool. Even though the mass and the stiffness distribution of a structure can be modeled within the FEM quite precisely, there is still a lack of suitable damping models. Classical approaches such as the Rayleigh damping or the identification of relaxation or creep functions by a Prony series result in a high frequency dependency of the damping properties which is in contrast to results from respective measurements [2]. Other approaches such as the use of fractional derivatives [3,4] are not available within commercial software programs. Another option offered by some FE codes is the 'constant hysteretic model' often introduced as 'structural damping'. This model assumes frequency independent damping properties, i.e. the hysteresis in a stress-strain diagram encloses the same area for all frequencies (and constant amplitude) [5,6]. Since the model leads to non-causal behavior in time-domain calculations [7] it can only be used in the frequency domain where one obtains a complex stiffness matrix. Thus, a modal analysis of a structure which incorporates hysteretic damping in general leads to complex eigenmodes and eigenvectors which have to be identified by a complex eigenvalue solver.
Depending on the location of a join patch within a structure, its contribution to the energy dissipation changes from mode to mode. This is why – in contrast to material damping – the damping properties of joints have to be modeled locally.

In this paper we consider a structure made of steel which includes two bolted joints. An EMA of the assembled structure is carried out to detect the eigenfrequencies, eigenmodes and the respective modal damping values. Then, a generic experiment is used to identify the tangential stiffness and the damping properties in terms of a loss factor of the join patches. Using these results, a FE model is set up in NASTRAN where the join patch is represented by thin-layer elements (TLEs) with orthotropic material behavior. The material parameters of the TLEs are calculated from the measured joint's tangential stiffness, an estimated normal stiffness and the damping properties from the generic experiment which are included in terms of the constant hysteretic model. A numerical modal analysis of the FE model is calculated and the results are compared with those obtained from the EMA. In order to get a further reduction of the deviation between experimental and numerical results, an optimization procedure based on the least-squares method is coded in Matlab where the normal stiffness, the tangential stiffness and the loss factor are taken as free variables.

2. STRUCTURE AND ITS FE MODEL

The structure under consideration consists of a hollow cylindrical body (wall thickness: 8 mm) with flanges on the ends, which is enclosed by two circular cover plates (10 mm thick), each mounted with 12 bolts (M8, see Figure 1). The contact surface between the flanges and the circular plates are modeled in the FEM by thin-layer elements (TLEs) with orthotropic material behavior. The model of constant hysteresis is used to model the damping resulting in complex-valued stiffness matrices of the TLEs.

In order to detect the tangential stiffness and loss factor of the joint, a so-called generic joint experiment is performed (see Figure 2). The set-up consists of two masses m_1 and m_2 connected by a lap joint, which has the same surface finish as the joints of the structure. The normal pressure is nearly constant due to a sufficient thickness of the lap. The normal force can be adjusted by the bolt and is measured by a piezoelectric washer. The normal force is adjusted to obtain the same contact pressure as in the assembly. Mass 2 is excited by an electro-mechanic shaker with a sine input signal. Once the vibration reaches a constant level, the accelerations a_1 and a_2 on both sides of the joint are acquired. These signals are integrated twice with respect to time to receive the absolute displacement. By taking the difference between them, the relative displacement in the joint is determined. The force transmitted by the joint is calculated as a product of the mass m_1 and its acceleration a_1. Knowing the transmitted force and relative displacement, a force-displacement diagram is constructed (see Figure 3) where the loss factor

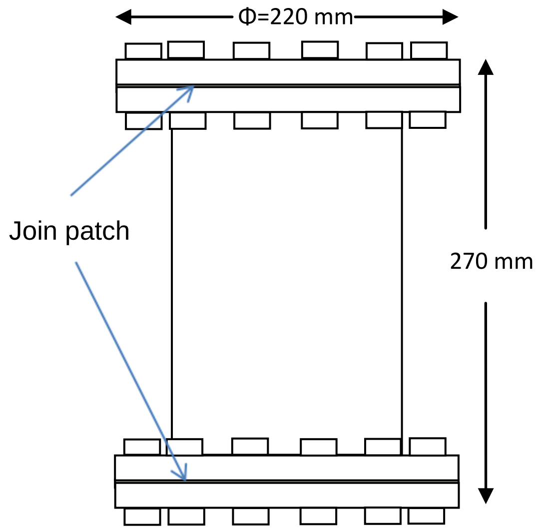

Figure 1 – Structure with bolted joints.

$$\eta = \frac{W_\mathrm{d}}{2\pi\, U_\mathrm{max}} \tag{1}$$

is calculated from the area W_d enclosed by the hysteresis curve (representing the dissipated energy) devided by the 2π-fold of the maximal stored energy U_max [8]. The slope of the hysteresis loop represents the tangential stiffness k of the joint.

The stiffness k from the generic joint experiment must be transferred into the FE model as a parameter of the TLEs. A schematic of an arbitrary joint with an TLE is depicted in Figure 4. The force F acting on both sides of the joint produces a shear stress τ in the TLE. This stress can be expressed as

$$\tau = G\gamma \approx G\frac{u}{d} \tag{2}$$

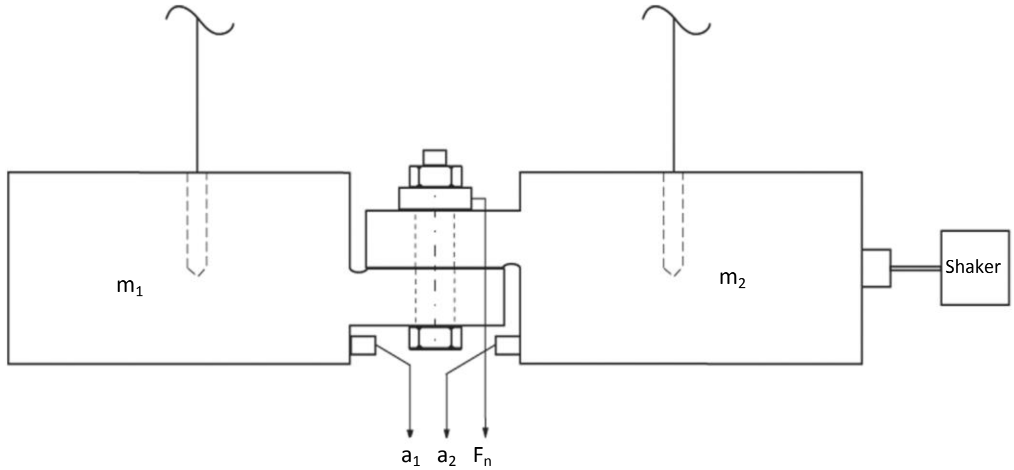

Figure 2 – Set-up of the generic experiment

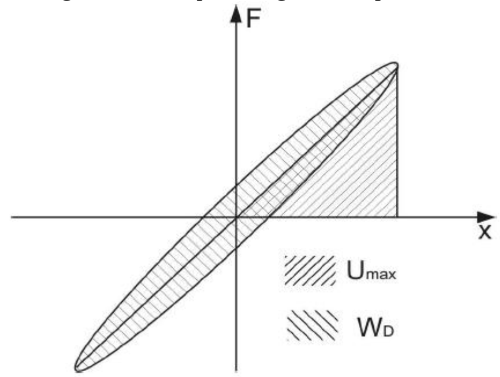

Figure 3 – Hysteresis curve

where G is the shear modulus, γ is the shear strain, u is the displacement and d is the thickness of the TLE. The shear stress can also be expressed as the ratio of the applied tangential force F and the area of the contact A

$$\tau = \frac{F}{A} \tag{3}$$

By combining Equations (2) and (3) the force can be calculated

$$F \approx \frac{GA}{d} u = ku \tag{4}$$

And from (4) one finally obtains

$$G = \frac{kd}{A} \ . \tag{5}$$

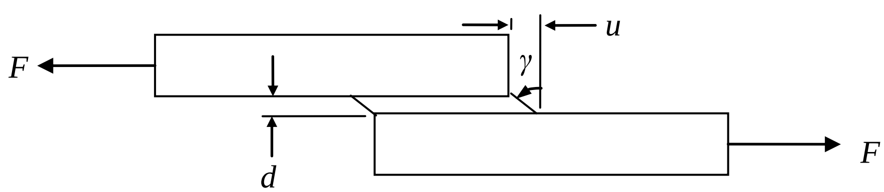

Figure 4 – Schematic joint

Since the join patch shows different stiffness and damping properties in normal and in tangential direction, an orthotropic material model has to be used for the TLEs. The respective material matrix reads

$$\begin{bmatrix} \sigma_{xx} \\ \sigma_{yy} \\ \sigma_{zz} \\ \sigma_{xy} \\ \sigma_{yz} \\ \sigma_{zx} \end{bmatrix} = \begin{bmatrix} E_{11} & E_{12} & E_{13} & 0 & 0 & 0 \\ E_{12} & E_{22} & E_{23} & 0 & 0 & 0 \\ E_{13} & E_{23} & E_{33} & 0 & 0 & 0 \\ 0 & 0 & 0 & E_{44} & 0 & 0 \\ 0 & 0 & 0 & 0 & E_{55} & 0 \\ 0 & 0 & 0 & 0 & 0 & E_{66} \end{bmatrix} \begin{bmatrix} \varepsilon_{xx} \\ \varepsilon_{yy} \\ \varepsilon_{zz} \\ \varepsilon_{xy} \\ \varepsilon_{yz} \\ \varepsilon_{zx} \end{bmatrix} \tag{6}$$

where z is the normal direction of the joint's interface. For the TLEs all off-diagonal terms in (6) vanish since no transversal contraction occurs within the contact surface. In addition, as the interface obeyes no stiffness in x- and y-direction, the terms E_{11} and E_{22} are zero. Since the joint also exhibits no stiffness for in-plane shearing, E_{44} vanishes as well.
E_{33} represents the normal stiffness, whereas $E_{55} = E_{66}$ define the tangential stiffness of the joint. The relations between E_{55} and E_{66} with the shear moduli G_{zx} and G_{zy} are

$$E_{55} = 2G_{zy} \quad \text{and} \quad E_{66} = 2G_{zx} \,. \tag{7}$$

For numerical reasons the values of E_{11}, E_{22}, and E_{44} entered in the NASTRAN must be different from zero but can be set to a value many magnitudes smaller than those for E_{33}, E_{55}, and E_{66}.

The eigenvalue problem of an undamped system with n degrees of freedom, the stiffness matrix $\boldsymbol{K}$ and the mass matrix $\boldsymbol{M}$ is given by

$$(\boldsymbol{M}\lambda_i^2 + \boldsymbol{K})\boldsymbol{\varphi}_i = 0 \,, \tag{8}$$

where λ_i are the n (real) eigenvalues and $\boldsymbol{\varphi}_i$ the respective (real) eigenvectors. Using the model of constant hysteresis, the equation is extended to

$$(\boldsymbol{M}\lambda_i^{*2} + \mathrm{i}\boldsymbol{D} + \boldsymbol{K})\boldsymbol{\varphi}_i^* = (\boldsymbol{M}\lambda_i^{*2} + \boldsymbol{K}^*)\boldsymbol{\varphi}_i^* = 0, \tag{9}$$

where the superscript $\cdot^*$ shall denote complex quantities. The damping matrix $\boldsymbol{D}$ is constructed from the TLEs as the real stiffness matrix $\boldsymbol{K}_{\mathrm{TLE}}$ derived from Eq. (6) multiplied by the loss factor η from the generic experiment, see Eq. (1). Thus, the complex stiffness matrix $\boldsymbol{K}_{\mathrm{TLE}}^*$ of a TLE reads

$$\boldsymbol{K}_{\mathrm{TLE}}^* = \boldsymbol{K}_{\mathrm{TLE}}\,(1 + \mathrm{i}\eta_{\mathrm{TLE}})\,. \tag{10}$$

The system matrices are then assembled from all element matrices. The first 20 complex eigenvalues λ^* and the respective eigenvectors $\boldsymbol{\varphi}_i^*$ are calculated in NASTRAN using the upper Hessenberg method.

3. EXPERIMENTAL RESULTS

The EMA of the assembled structure is performed up to 4.5 kHz and 14 modes are identified through this range of frequency. The eigenfrequencies and the respective modal damping values are given in Table 1. Due to the symmetry of the structure double modes appear except for modes 5 and 6.

The generic joint experiment is performed in a frequency range from 200 Hz up to 1500 Hz. In order to stay well below the first eigenfrequency of the experimental set-up, measurements at higher frequencies are not carried out. Since the identified stiffnesses and loss factors does not change notably with the frequency, the assumption of a constant hysteresis is confirmed. The identified values are

$$k = 520 \ \frac{\mathrm{kN}}{\mathrm{mm}} \quad \text{and} \quad \eta = 0.028, \tag{11}$$

where especially the loss factor shows some uncertainty which can be seen if the measurement is repeated with the same contact pressure and excitation after the set-up of the generic experiment is unmounted and re-assembled.

Table 1 – Experimental eigenfrequencies and modal damping

Eigenfrequency number	Eigenfrequency (Hz)	Modal damping [%]
1	2038	0.06979
2	2084	0.06979
3	2809	0.07633
4	2874	0.07633
5	2961	0.3135
6	3277	0.3012
7	3986	0.1369
8	3988	0.1369
9	4242	0.113
10	4251	0.113
11	4353	0.1369
12	4353	0.1369
13	4462	0.03198
14	4462	0.03198

4. FE RESULTS AND OPTIMIZATION

A FE modal analysis is carried out where the structure is discretized with more than 250000 dof by 8-noded brick elements. Neither the bolts nor the holes are included in the FE model. The thickness of the TLEs is chosen as d=0.1 mm. Since the contact area A=1087 mm² of the generic experiment is known, the entries of the material matrix can be calculated from (5) and (7) as

$$E_{55} = E_{66} = 95.7 \, \frac{\mathrm{N}}{\mathrm{mm}^2} \; . \tag{12}$$

Since no measurements of the normal stiffness are available, E_{33} is estimated to 5000 N/mm². The material data for the structure itself (steel, isotropic) is taken to be $E = 207500\ \mathrm{N/mm^2}$ for the cylinder, $E = 210000\ \mathrm{N/mm^2}$ for the cover plates, density $\rho = 7790\ \mathrm{kg/m^3}$, and Poisson's ratio $\mu = 0.3$.
A comparison between the measured and the calculated eigenfrequencies of the first 12 modes shows a mean absolute deviation of 1.8 %. However, the calculated modal damping values are notably underestimated. Possible reasons are the negligence of material damping, energy dissipation into the surrounding air and the simplified modeling of the bolts. I.e. all contact surfaces of the 24 bolts and the screw nuts are neglected but also the threads of the scews are in contact with the nuts and possibly also with the bored holes of the structure.

In order to obtain better results, a model-updating procedure is coded in Matlab, where the loss factor, normal and tangential stiffnesses of the TLEs are taken as free variables. This optimization is run with the 'lsqnonlin' command in Matlab which minimizes the residuum r from the measured and the calculated data (eigenfrequencies f_i and percentage modal damping η_m) in a least-squares sense for non-linear problems

$$r = \sum_i \left(f_i^{\mathrm{exp}} - f_i^{\mathrm{FEM}}\right)^2 + \left[w\left(\eta_{\mathrm{m},i}^{\mathrm{exp}} - \eta_{\mathrm{m},i}^{\mathrm{FEM}}\right)\right]^2 = \min. \tag{13}$$

Since the modal damping values are by some orders of magnitude smaller than the eigenfrequencies, a weighting factor $w = 100$ is introduced. During the optimization, Matlab runs the program NASTRAN with different sets of parameters to test the sensitivity of the residuum r on the three parameters and then reduce it step by step. The whole procedure takes some hours as each numerical modal analysis in NASTRAN lasts more than 10 minutes.

Special care has to be taken due to the swapping of modes in the numerical calculation for different sets of parameters. In order to compare the eigenfrequencies and damping values of the same modes (measured and calculated) in Eq. (13) a special routine is coded in Matlab which identifies the calculated eigenmodes and refers them to the corresponding measured eigenmodes.
The optimization results (TLE parameters) are the normal stiffness $E_{33} = 786\ \mathrm{N/mm^2}$, the tangential stiffness $E_{55} = E_{66} = 956\ \mathrm{N/mm^2}$ and the loss factor $\eta = 0.0590$. According to these parameters, the average deviation for the eigenfrequencies is 1.03%. The average deviation for the modal damping values is 28.13% which is a good result considering the uncertainties in the experimental work and the simplification in the FE model. The resulting eigenfrequencies and modal damping measures of the optimization are given in Tables 2 and 3. In Figures 5 and 6 the respective results are displayed graphically.

Table 2 – EMA and FEM results for the eigenfrequencies

	Eigenfrequency (Hz)		
Eigenfrequency number	EMA	FEM	Difference (%)
1	2038	2083.8	2.2483
2	2084	2084.1	0.029311
3	2809	2908.5	3.5609
4	2874	2915.5	1.4371
5	2961	2930.4	-1.0307
6	3277	3255.3	-0.67335
7	3986	4011.3	0.63486
8	3988	4011.4	0.58796
9	4242	4227	-0.35248
10	4251	4227.2	-0.55958
11	4353	4348.5	-0.10368
12	4353	4348.6	-0.10086
13	4462	4524.9	1.4335
14	4462	4536.1	1.6841

Table 3 – EMA and FEM results for the modal damping

	Modal damping [%]		
Eigenfrequency number	EMA	FEM	Difference (%)
1	0.06979000	0.11592	66.092
2	0.06979000	0.11588	66.043
3	0.07633000	0.054337	-28.812
4	0.07633000	0.054208	-28.981
5	0.31350000	0.31001	-1.1124
6	0.30120000	0.29173	-3.1449
7	0.13690000	0.091385	-33.247
8	0.13690000	0.091355	-33.269
9	0.11300000	0.061808	-45.303
10	0.11300000	0.061816	-45.296
11	0.13690000	0.16116	17.718
12	0.13690000	0.16114	17.709
13	0.03198000	0.033143	3.637
14	0.03198000	0.0331	3.5007

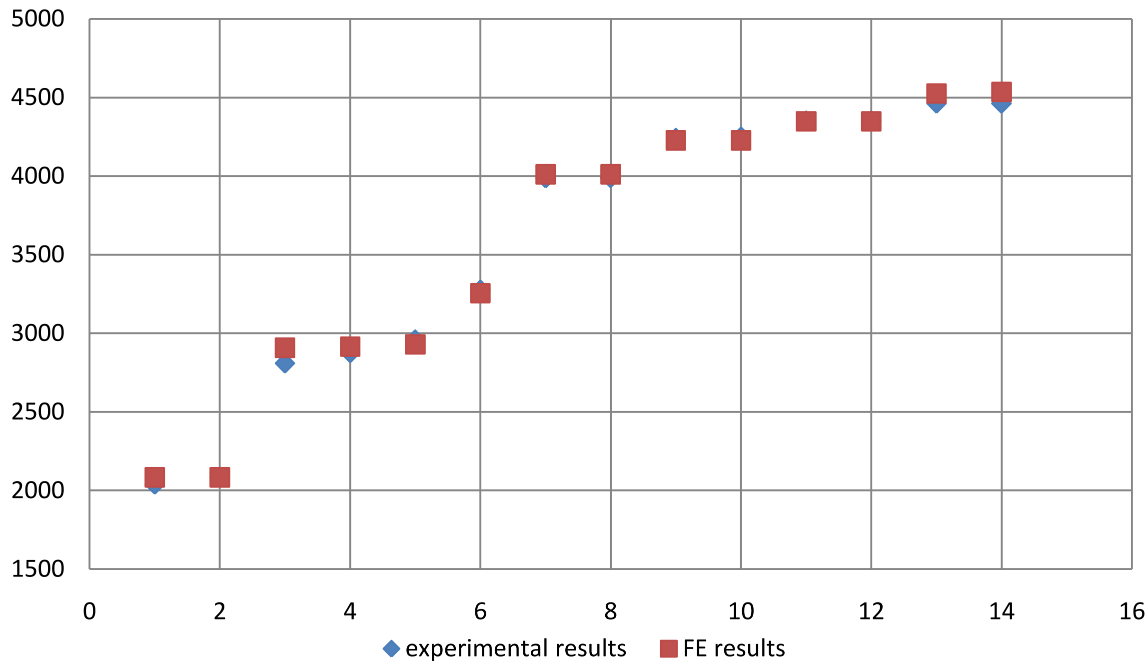

Figure 5 – Eigenfrequency vs. mode number

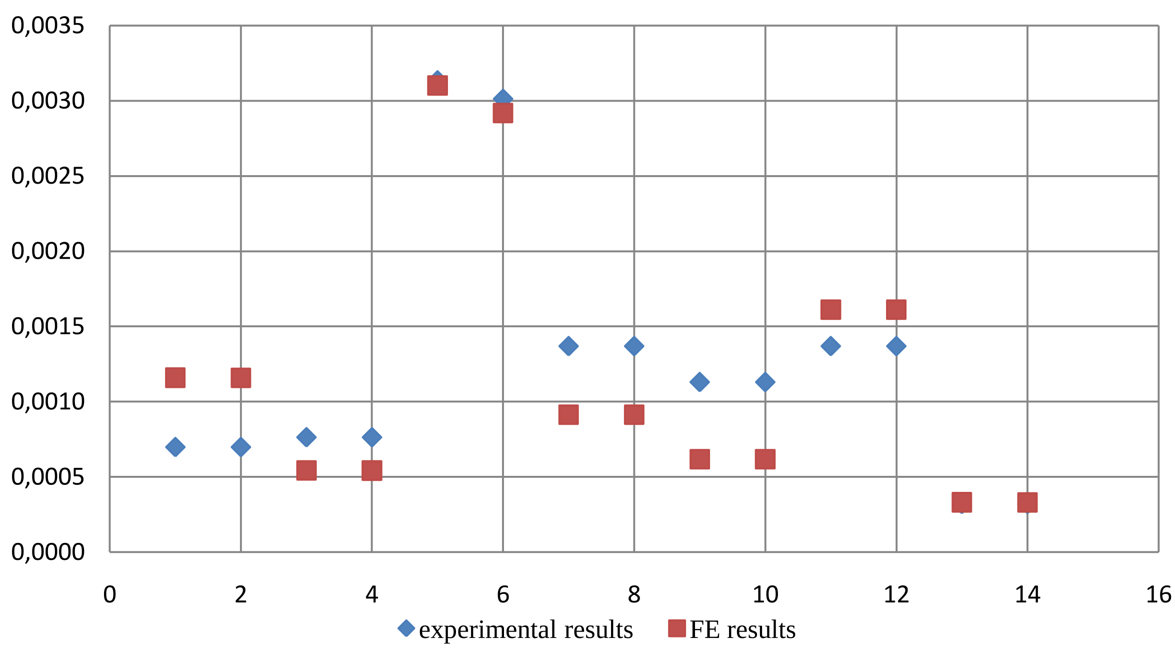

Figure 6 – Modal damping vs. mode number

5. CONCLUSIONS

Using the model of constant hysteresis in conjunction with thin-layer elements for finite element calculations leads to good results when the damping properties of assembled structures are investigated. This approach allows to model the damping locally and thus results in complex eigenvalues and eigenvectors. In contrast to global damping models, modes with high or low modal damping values can be identified. This fact can be essential, if the crucial (low-damped) eigenfrequencies of a structure shall be identified in the design phase in order to modify the construction before any prototype is produced. While the eigenfrequencies and the eigenmodes can be predicted by the FEM to a high degree of accuracy, the predicted damping values may notably differ from measured values. This is due to many uncertainties in the FE model but also a result of significant scattering of measured damping values. Nevertheless, a qualitative prediction of modes with high damping and lowly-damped modes is possible.

The constant hysteretic damping model obviously fits measured data much better than classical models such as the Rayleigh damping or other approaches with velocity-proportional damping forces. The model needs only one parameter (for a 1d problem) which can easily be identified. However, time-domain calculations are not possible with this damping model since it leads to non-causal behavior.

The generic experiment is a good way to find a first approximation for the stiffness and the energy losses in joints of assembled structures but the parameter optimization (model updating) reveals a potential for further improvement.

ACKNOWLEDGEMENTS

The financial support of the DFG (Deutsche Forschungsgemeinschaft) and the FVV (Forschungsvereinigung Verbrennungskraftmaschinen) is gratefully acknowledged. We also like to thank Atlas Copco for their cooperation and the fabrication of the test specimens and the investigated structure.

6. REFERENCES

[1] Gaul, L., Schmidt, A., Bograd, S., “Joint damping prediction by thin layer elements”, Proceedings of IMAC XXVI: A Conference & Exposition on Structural Dynamics, Orlando, FL, USA, February 4-7, 2008, CD-ROM.

[2] Bathe, K. J., “Finite Element Procedures”, Prentice Hall, 1995.

[3] Oldham, K. B., Spanier, J., “The Fractional Calculus”, Academic Press, 1974.

[4] Lakes R. S. “Viscoelastic Solids”, CRC Press, 1999.

[5] Ganapathi, M., Patel B.P., Boisse, P., Polit, O. “Flexural loss factor of sandwich and laminated composited beams using linear and nonlinear dynamic analysis”, Composites: Part B, 30, 1999, pp. 245-256.

[6] Chen, X., Chen, H. L., Hu, X. L., “Damping prediction of sandwich structures by order-reduction- iteration approach”, Journal of Sound and Vibration, 222(5), 1999, pp. 803-812.

[7] Gaul, L., Bohlen, S., Kempfle, S., “Transient and forced oscillations of systems with constant hysteretic damping”, Mechanics Research Communications 12 (4), 1985, pp. 187-201.

[8] Thorby, D., “Structural Dynamics and Vibration in Practice”, First edition, Elsevier, 2008.